2017-01-01

AC Susceptibility And EPR Investigations Of Superspin Dynamics In Manganese Oxide Nanoparticles

Mahesh Koirala
University of Texas at El Paso, mkoirala@miners.utep.edu

AC SUSCEPTIBILITY AND EPR INVESTIGATIONS OF SUPERSPIN DYNAMICS IN MANGANESE OXIDE NANOPARTICLES

MAHESH KOIRALA

Master's Program in Physics

APPROVED:

Cristian E. Botez, Ph.D., Chair

Russell R. Chianelli, Ph.D.

Rosa Fitzgerald, Ph.D.

Charles Ambler, Ph.D.

Dean of the Graduate School

Dedication

To my parents

Madhu and Saraswati Koirala

for their love, friendship, and support.

AC SUSCEPTIBILITY AND EPR INVESTIGATIONS OF SUPERSPIN DYNAMICS IN MANGANESE OXIDE NANOPARTICLES

by

MAHESH KOIRALA

THESIS

Presented to the Faculty of the Graduate School of

The University of Texas at El Paso

in Partial Fulfillment

of the Requirements

for the Degree of

MASTER OF SCIENCE

Department of Physics

THE UNIVERSITY OF TEXAS AT EL PASO

August 2017

Acknowledgements

I would like to thank Dr. Cristian E. Botez for his guidance of my research work, his suggestions throughout the project, and for the opportunities he has given to me. I would like to express my gratitude towards Dr. Russell Chianelli and Dr. Rosa Fitzgerald for their help regarding this thesis. My thanks to Alex D price, Dr. Alan Goos and Dr. Sohan de Silva for their assistance and guidance in various aspects of this research. My special thanks to my friends and family, for their love, friendship, and encouragement. I would also like to extend a special thank you to my wife Manisha Poudel and friends Pawan Koirala and Kamal Nyaupane for their support and irreplaceable friendship.

Abstract

We have investigated the superspin dynamics of 5 nm and 10 nm mixed state Mn_3O_4 nanoparticles utilizing ac-susceptibility and electron paramagnetic resonance measurements. The out of phase component of the ac-susceptibility measurements show a magnetic anomaly below ($T<T_N$) the paramagnetic to ferrimagnetic transition ($T_N \cong 41K$) of the selected material. EPR spectra show markedly different magnetic signatures which corroborate the particle size dependence as shown in the low-temp ac-susceptibility scans, both of which depict superparamagnetic behavior.

Table of Contents

List of Figures

Chapter 1: Introduction

Nanoscience, in general, is defined as the study of physical properties of materials and phenomena when the particle size is on the scale of 1 – 100 nm. The magnetic domains within the material are responsible for the various behaviors magnetic materials exhibit. In recent studies of science and technology, magnetic nanoparticles are showing potential in the development of high-density storage [1] and in biomedicine, such as cancer treatments.

1.1 Magnetic Nanoparticles

Magnetic nanoparticles are trending topics in research due to their interesting properties most important of which is due to their size. Many unique and important behaviors arise in magnetic nanoparticles below some critical size.

Before some decades it has been the matter of important research that how magnetic nanoparticles interacts [2]. Although many research are being done mainly to understand the properties of magnetism, recent research in magnetic nanoparticles are based in two main industries/ the electrical industry/ computer sciences [3] and the biosciences [4].

The most important thing in electronics industry and computer sciences is producing higher density magnetic storage media. Making faster and smaller data storage material are key points today [5].

Magnetic hyperthermia (cancer treatment), and magnetic immunoassay (using magnetic beads for diagnosis) [6-7] are among the variety of applications of magnetic nanoparticles in biosciences. The use of magnetic nanoparticles in biosciences includes magnetic imaging

technique, controlling key magnetic properties, chemical binding properties and reliable dispersion mechanism.

Eventually it is important to study different types of behavior present in magnetic nanoparticles such as transitions, relaxations, reversal dynamics and understand the chemical behaviors that forms such behaviors which helps to operate such system for our benefits. Therefore many discoveries and theories have been established to explain the intrinsic properties of magnetic nanoparticles.

1.2 Manganese Oxide

Due to wide application of metal oxide in energy storage, magnetic storage sensors and ferrofluids, manganege oxide (MN_3O_4) are used as main source of ferrite material and applied mainly in magnetic and electrochemical catalysis [8]. Using various methods such as ultrasonic gamma and microwave irradiation, thermal decomposition its compound shows different shapes including nanoparticles, nanorods, nanowires and tetragonal particles. They occur in mixed oxidation state of +2 and +3. The main application of MN_3O_4 includes catalysts, ion-exchange materials, electrochemical materials, high-energy magnetic storage media, solar energy transformation, molecular absorption etc. [9].

Chapter 2: Theoretical Background

2.1 Magnetization

To explain the magnetic behavior of manganese nanoparticles it is useful to study about some known type of magnetic behavior. Also the cause and effect of magnetism is explained in summary.

The combination of electrons orbital momentum and intrinsic spin forms a magnetic dipole resulting in a magnetic field so the basic origin of magnetism is from electrodynamics and quantum mechanics. While nucleons or any other particle with electric charge are theoretically assumed to generate magnetism, there net contribution is so negligible that can usually be neglected. The magnetic field created follows the superposition principle [10] and within the material every particle producing a magnetic field is successively inducing and being induced magnetically by every other particle generating a magnetic field. Therefore a self-motivated magnetic system can be developed in a material.

Consider two dipoles in close vicinity, and then we expect two dipoles always align in opposite direction but when we take the Pauli Exclusive Principle [11] for electrons this is not true. In fact when the dipoles aligns parallel, it would decrease the electrostatic interaction energy than compared to the dipoles that are aligned anti parallel. This can be explained by exchange interactions and the difference is known as exchange energy.

The quantum mechanical phenomenon that explains the change of the expectation value of energy or the distance between two identical particles due to wave function overlap is basically called the exchange interactions. This is the main reason of assembling of atomic magnetic moments in magnetic solids.

The main thing that needed to be addressed now is the material's magnetization, which is proportional to the magnetic moment of the particle. The measure of the strength and direction of the magnetization of the material is the magnetic moment.

The other term related with the quantity of magnetization of a material that counters to an applied magnetic field is Magnetic Susceptibility, which is given by:

$$M = \aleph H \qquad (1)$$

Where M is magnetization, $\aleph$ is magnetic susceptibility and H is the magnetic field strength. Materials are classified according to their magnetic susceptibility. If the material has negative susceptibility it is diamagnetic, if positive susceptibility it is paramagnetic.

2.1.1 Magnetic Domains

Magnetic domain is a region within a magnetic material consisting of a magnetization in a uniform direction, the net magnetization of which follows superposition principle. Magnetization with a coherent rotation between the two magnetic domains is enclosed within a region called domain wall, which is space between magnetic domains. In the absence of external field the sample has no magnetization and magnetic domains are randomly oriented. When magnetic field is applied the magnetic domains are associated in certain direction and net magnetization of the material is registered as shown in fig 2.1.

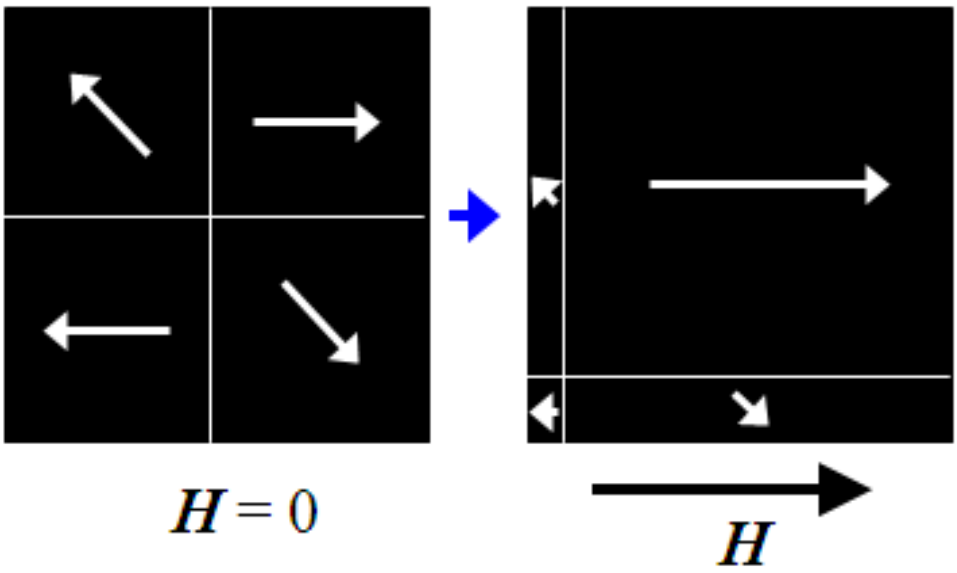

Figure 2.1 – Magnetic Domain Behavior

2.1.2 Diamagnetism

Diamagnetism is the weak form of magnetism which response opposite to the applied external field. It is the property of all material. Diamagnetic materials lack unpaired electrons and atom or molecules, which eventually make it with no any angular momentum so the magnetization due to an external field is the property of electrons orbital motions

2.1.3 Ferromagnetism

Ferromagnetic materials are the magnetic materials, which becomes magnetized upon the application of an external magnetic field and remains magnetized on the removal of magnetic field. Ferromagnetism is one of the oldest known forms of the magnetism. Horse shoe magnets and bar magnets are the good examples of ferromagnetic objects. In ferromagnetism all the ions

within a ferromagnetic material add a positive contribution to the net magnetism whereas, in ferrimagnetic there is some decline in the alignment resulting lower net magnetism as some magnetic moments align oppositely. Further, in antiferromagnetic material almost all ions subtract from the net magnetization resulting total magnetic field is zero [12]. All the explained terms are shown in figure 2.2

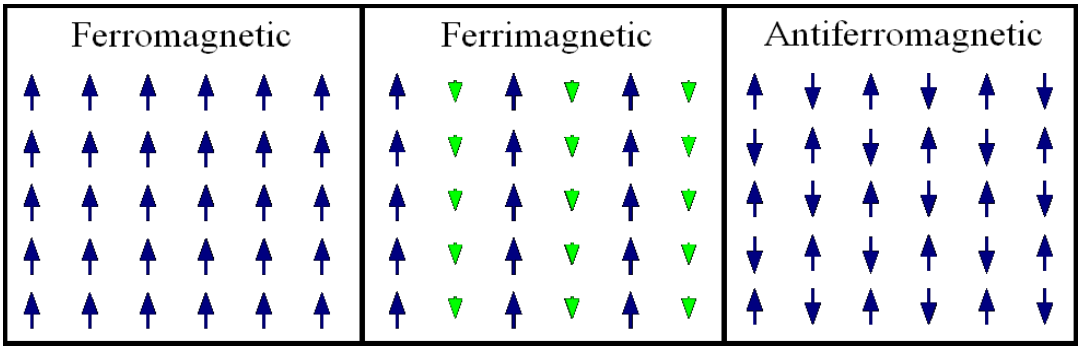

Figure 2.2 – Ferromagnetic, Antiferromagnetic, and Ferrimagnetic Behavior

Ferromagnetism shows its properties within a certain temperature range only. This temperature range is called Curie temperature. If the ferromagnetic material surpasses the Curie temperature it will loose its ferromagnetic properties. This is due to the overcome of dipole interaction energy by internal thermal energy resulting dipoles to move without restriction and align within the material above the temperature range.

2.1.4 Paramagnetism

Another type of magnetism familiar to most is Paramagnetism. It is the form of magnetism in which all the magnetic domains aligns parallel to the external magnetic field but in the absence of external magnetic field magnetic domains do not exist and there is no net magnetism.

In paramagnet when there is no external field, interaction energy between the dipoles is overcome by internal thermal energy as a result of which there is no ordering of the domains. All the domains are moving randomly in an independent manner and do not interact with each other.

2.1.5 Superparamagnetism

Ferromagnetic materials in critical small size, basically at nano scale shows some interesting behavior, which is known as superparamagnetism. In nanoscale magnetic the magnetic moment will align within a particle, in their entirety, in the same direction. Each particle acts a single magnetic domain having its own magnetic moment. At some temperature like paramagnets the single domains rotates freely and align with an external field. Moreover, below this temperature the particle will be unable to rotate freely and said to be blocked. This behavior is referred as superparamagnetism[13].

2.1.6 Superparamagnetic Blocking

The temperature at which the single domain magnetic nanoparticles changes from its blocked state to a freely rotating super paramagnetic state is called blocking temperature.

$$T_B = \frac{KV}{k_B ln\left(\frac{\tau_m}{\tau_0}\right)} \qquad (2)$$

Where K is the nanoparticle's magnetic anisotropy energy density, V is the volume, k_B is the Boltzmann constant, τ_m is the measurement time, and τ_0 is the attempt time which is

characteristic of the material typically with a value of 10^{-9} - 10^{-12} seconds. The quantity KV is the energy barrier. The measurement time is observed in conjunction with the Neel relaxation time, τ_N, which is the mean time between impulsive flips between the magnetic moments. If the measurement time is above the relaxation time the material is in superparamagnetic state and in the reverse case it is in a blocked state.

2.1.7 Spin Glass

A material with a messy arrangement of magnetic moments is called a spin glass. It is identical to that of a chemical glass but in the place of position disorder there is spin configuration. So with ferromagnetism or anti-ferromagnetism no long range can be established due to this frozen-in structure disorder [14]. So in the absence of external field net magnetization is zero because of such disorder in the magnetic moments. Likewise similar type of disorder is found in a paramagnet but instead of dynamic disorder there is static disorder.

2.1.8 Super-Spin Glass

Super spin –glass to a spin glass relationship is similar to that of superparamagnet to a paramagnet. The super spin-glass behavior is similar to that of a spin-glass only difference is with the constitute particles. The constituent particles are single domain ferromagnetic clusters in super spin-glass whereas; in spin glass it is just the atomic dipoles [15].

2.2 Magnetic Behavior

Magnetic behavior of the material depends upon the electronic configuration of the material and expressed in terms of energy barriers/constraints. The material would exhibit new type of magnetic behavior if the enough thermal energy were supplied to the material to nullify

these barriers/constraints. Eventually we have then magnetic transitions, which are material specific with their corresponding transition temperature.

Many theories are involved with the magnetic phase and magnetic phase transitions. Good indicator for a particular magnetic system/transition is that the date can be acceptable to a corresponding mathematical model but this alone cannot confirm a particular type of magnetic system. There are numerous models but here we focus into those that are related to our study of nanoparticles.

2.2.1 Curie Law

During the study of magnetism Pierre Curie experimentally discovered the theory, which is known as Curie's Law that shows the temperature dependence of paramagnets

$$\boldsymbol{M} = C * \frac{\boldsymbol{B}}{T} \tag{3}$$

Where B is the magnetic field, T is the absolute temperature, M is the net magnetization and C is the curie constant of the material. From this equation, it can be explained that the magnetization is directly proportional to the applied field and inversely proportional to temperature. But this law holds only for high temperature or weak magnetic field. At low temperature thermal energy will be low to produce magnetic disorder and at high field magnetic moments will align in the direction of applied field.

2.2.2 Curie and Néel Points

Besides the effect of the distance the magnetic dipoles alignments and interaction are effected also by thermal oscillations or entropy. They can overcome the tendency for alignment.

Coupling force between the dipoles in the ferromagnets is overcomed by the enough thermal energy. So the temperature, which increases both thermal oscillations and entropy, is responsible for magnetic alignment of the material

This temperature, which describes the transition between two types of magnetic performance in ferromagnets, is called Curie temperature. Below Curie temperature a ferromagnet , as described in its definition have non zero magnetic field when there is external field. However above Curie temperature in the absence of external field the thermal energy is enough for the random orientations of the magnetic dipoles causing net magnetization zero. Hence Curie temperature describes the transition from ferromagnetism to paramagnetism. Similarly the transition from atniferromagnrtism to paramagnetism is described by Neel temperature

2.2.3 Néel – Brown Theory

Neel-Brown theory is an important theory to deal with the particles that show superparamagnetism. It is also called Neel- Arrhenius theory or Neel relaxation theory. The theory was first developed by Louis Neel [16] and further refined by William Brown [17]. This theory explains the magnetic response of single- domain ferromagnets. As already explained the particles are single domain, each particle acts as a single domain immense magnetic moment.

The magnetic anisotropy of the nanoparticle separates the steady alignments of the magnetic moment by an energy barrier. These steady alignments are defined by an “easy axis”, which is a material’s natural alignment of the magnetic moments, which is the favored alignment of spontaneous magnetization. The energy needed to change the direction of magnetization is called the energy barrier, by changing the direction of magnetization from an “easy axis” through

a “hard axis” and resting at another “easy axis”, and is dependent on material specific properties as well as the particle size. Therefore, when the size of the nanoparticle change, so does the energy needed to overcome the energy barrier, subsequently the critical temperature, at which the material shows superparamagnetic behavior.

The Néel – Arrhenius equation is used to measure the average length of time it takes for a ferromagnetic moment to arbitrarily flip due to the thermal oscillations in the material:

$$\tau_N = \tau_0 e^{\left(E/k_B T\right)} \quad (4)$$

Where τ_N is the average time for the spin to flip due to thermal oscillations, τ_0 is a constant called the attempt time, a characteristic of the material that is generally of the order $10^{-9} – 10^{-12}$ s, E is the magnetic anisotropy energy, k_B is the Boltzmann constant, and T is the absolute temperature. The energy barrier E= KV, where K is the anisotropy energy density and V is the volume, which shows energy barrier depends on particle size. Therefore as the particle size increase so does the energy needed to change its magnetic alignment, which leads to longer transition time from magnetic orientation with the recently applied external field to a randomized alignment

Above a certain temperature known, as the blocking temperature thermal energy is sufficient to allow the nanoparticles readily align with an external applied field. In this state the particle act like a paramagnet with huge moment, which state is known as super paramagnetic state. However below this critical temperature also known as blocking temperature, the nanoparticles will not be responsive enough to the applied field. This state is known as the blocked state.

2.2.3 Vogel-Fulcher Law

The law that describes magnetic relaxation is the Vogel – Fulcher activation law, which is analogous to the Néel – Arrhenius equation. This was suggested by Shtrikman and Wohlfarth [18] and by Tholence [19] as a model for spin glass relaxations.

The major modification between these equations is the Vogel – Fulcher activation law does account for some slight inter-particle interaction, making it useful for weakly interacting systems. The Vogel – Fulcher equation takes on a form analogous to that of the Néel – Arrhenius equation:

$$\tau = \tau_0 e^{\left(E/(k_B(T-T_0))\right)} \tag{5}$$

Where τ is the average time taken for a spin to flip directions due to thermal oscillations, τ_0 is the attempt time, E is the magnetic anisotropy energy, k_B is the Boltzmann constant, T is the absolute temperature, and T_0 is the material specific characteristic temperature which accounts for the inter-particle interactions.

2.2.4 Power Law

At high particle concentration, the effects of inter-particle interaction have an effect on the magnetic phase shift about the Curie point. Instead of blocking, the superspins freeze in a spin-glass fashion when cooled below a critical temperature [20-21]. This power activation law will be momentarily explained.

Conformist dynamic scaling theory describes that the relaxation time τ for a system deviates as a power law with the correlation length ξ, such that $\tau = \tau_0 \xi^z$, where z is the dynamic scaling exponent. The correlation length is defined as a parameter that deals with the average magnetic domain size. As explained by static scaling hypothesis, parameters such as the correlation length and time should diverge, and the magnetization should reduce correspondingly to the value of the reduced temperature to the related dynamic exponent. The correlation length becomes defined as:

$$\xi = \left(\frac{T}{T_G} - 1\right)^{-\nu} \tag{6}$$

Where ξ is the correspondence length, T is the temperature, T_G is the material particular spin-glass freezing temperature, and ν is a critical exponent. Joining this with the base form for the power law, the power law takes on the form:

$$\tau = \tau_0 \left(\frac{T}{T_G} - 1\right)^{-z\nu} \tag{7}$$

where $z\nu$ becomes the critical exponent. This power law is used for data fitting, just as the Néel – Arrhenius and Vogel – Fulcher equations are used.

Where $z\nu$ becomes the critical exponent. This power law is used for data fitting, just as the Néel – Arrhenius and Vogel – Fulcher equations are used.

Chapter 3: Experimental Methodology

3.1 Single Crystal X-ray Diffraction

X-ray crystallography is one of the most important achievements for the study of molecular and atomic structure of a crystal. With the measurement of angles and intensity of the diffracted beam various information of the crystal can be studied.

Single crystal X ray diffraction can be taken to determine average size of the crystal. When X ray beam is sent directly through the sample generating an increasing cone (Debye-Scherrer) radially outward from the sample at every angle (2θ). Consequently a 2-d arrangement is gathered by a flat panel detector on the side opposite the x-ray beam, made up of concentric rings of changing intensity fig 3.1. Each ring corresponds to a particular reciprocal lattice vector *G* in the sample crystal, which is due to taking consideration of Bragg's law.

$$G = q = 2\,k\,\mathrm{Sin}\,[\theta] = 4\,\pi\,\mathrm{Sin}\,[\theta] / \lambda \qquad (8)$$

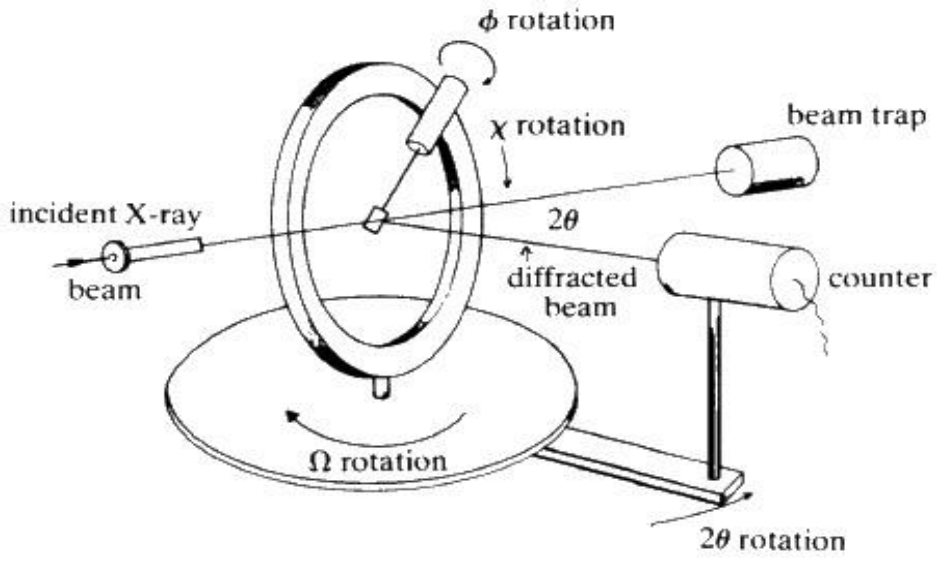

Figure- 3.1 Single Crystal X-ray Diffraction

Now using the Debye-Scherrer formula we determine the average nanoparticle size. The Debye-Scherrer formula connects average nanoparticle size to the width of clear intensity peaks (since intensity is measured as a function of two theta), the shape factor (a constant based of the geometry of the particles), and the wavelength of the incident X-rays [22].

3.2 Electron Paramagnetic Resonance

The technique which is based on the absorption of electromagnetic radiation, usually in the microwave frequency region by a paramagnetic sample placed in an external magnetic field is called electron paramagnetic resonance (EPR). Exciting the electron spins of unpaired electrons causes EPR. Every electron has a magnetic moment and half integer spin, with the magnetic components $m_s = \pm ½$. The electrons associate in either a parallel or antiparallel fashion with the field in the presence of external field. These configurations have specific energies tied to them due to the Zeeman effect given by:

$$E = m_s g_e \mu_B B_0 \tag{8}$$

where E is the energy, m_s is the spin value, g_e is the g-factor (typically around 2 and equal to 2.0023 for the free electron [23]), μ_B is the Bohr magneton, and B_0 is the strength of the magnetic field. Unpaired free electrons have separation energy of

$$\Delta E = g_e \mu_B B_0 \tag{9}$$

thus splitting of energy level is proportional to the magnetic field . The photons have energy of *hv*, the absorption or emission of a photon at resonance $hv = \Delta E$ permit the unpaired electron to move between the two energy levels. The resonance position can then be given by

$$B_0 = \frac{h\nu}{g_e \mu_B} \tag{10}$$

In fact, the frequency of the incident photons is held constant and the magnetic field is varied. As Maxwell-Boltzmann distribution explains electron esteems lower energy state, there is a clear absorption from the sample which is what becomes transformed into EPR spectrum.(figure 3.2)

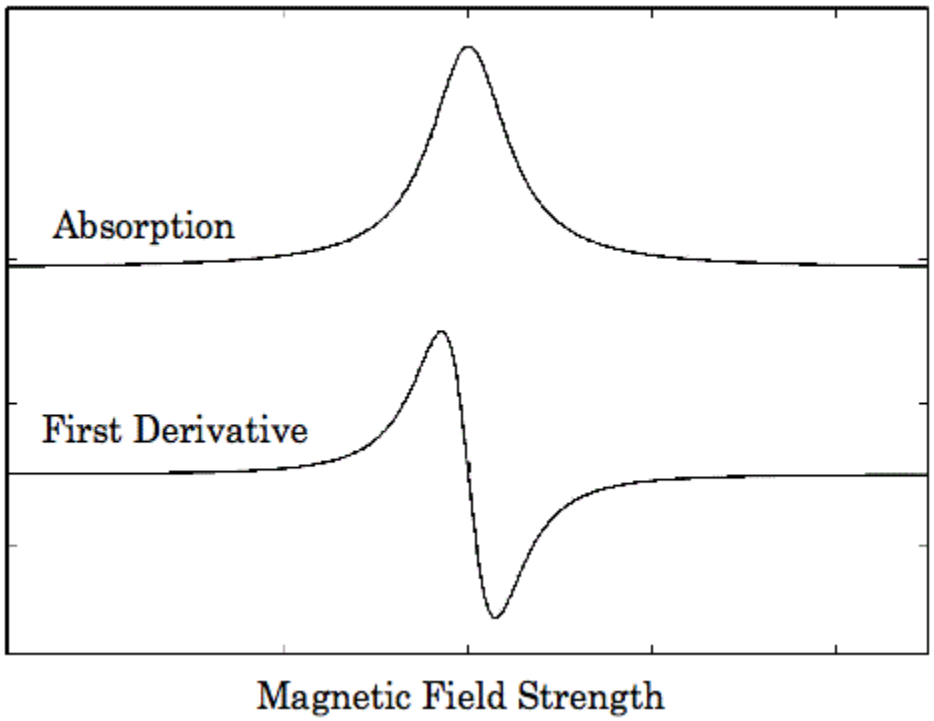

Figure 3.2 – Example of EPR Absorption Spectra and its First Derivative

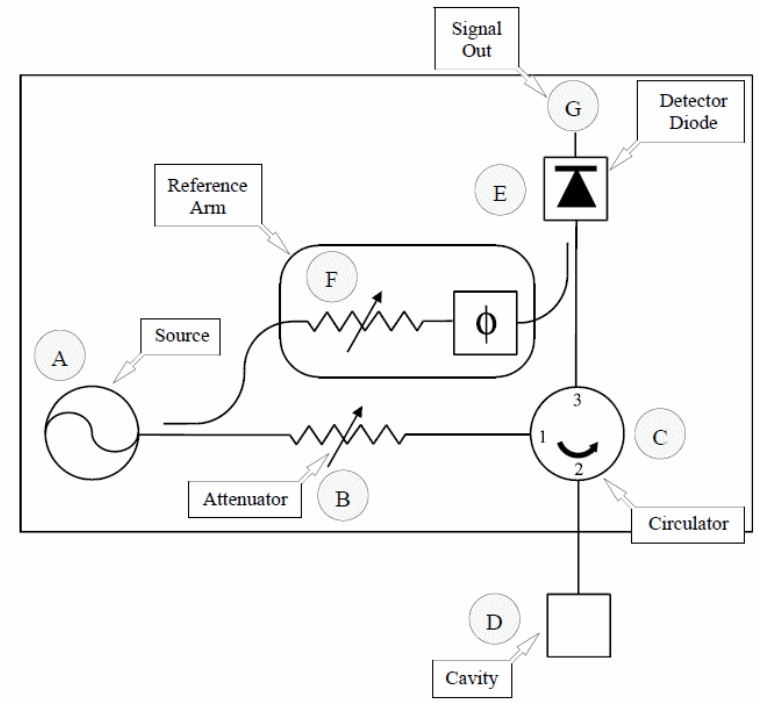

Figure 3.3 – Block Diagram Example of EPR Microwave Bridge

Figure 3.3 shows the microwave bridge for an EPR system. The opening point is the source marked by point A. Adjustable attenuator (point B) is used to control the power of the microwave, which reach the sample. A circulator (point C) permits microwaves to go to the sample (point D) not to the detector and the reflected microwaves to go to not to the source. The reflected microwave power is transformed into an electrical current by the Scotty barrier diode (point E). The proper current for smooth operation is retained by the reference arm (point F), which taps some of the source microwave power and sends it to the detector diodes. Another attenuator placed there controls the amount of power sent to the diode detector. Also the phase shifter assures the reflected signal combines appropriately with the supply signal.

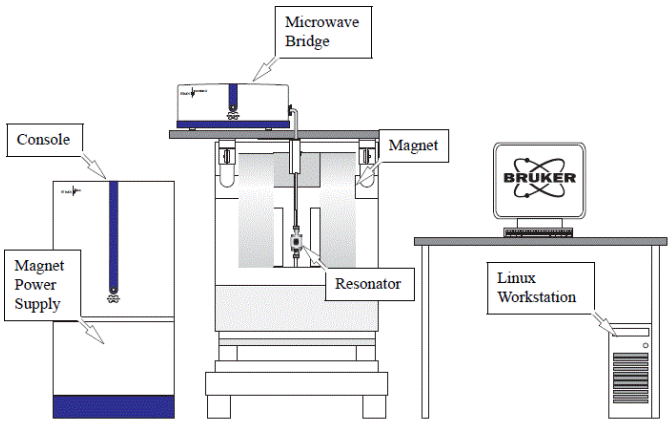

Figure 3.4 – Modules and Components of the Bruker EMXplus Spectrometer

Figure 3.4 shows Bruker EMX-plus X-band spectrometer where measurement was carried out. The microwave source has a constant frequency of 9.398 GHz (X-band). Mn_3O_4 in the powder form was lowered into the resonator and cooled to 20 K. The magnetic field was varied from 0G to 6000 G and the scan was taken. We then increased the temperature by 10 K, permitting abundant time (about 10 – 15 minutes) for the sample to come to thermal equilibrium with the resonator chamber, repeating this process until we spanned the 20 K – 80 K temperature range.

3.3 Magnetometry

Initially the term magnetometer was known, as 'magnetometer' was an instrument for measuring the earth's magnetic field [22]. At present any scientific instrument used for measuring magnetic field is referred as Magnetometry. In study of modern scientific technique Magnetometry is used to measure magnetization and magnetic related properties either in room temperature and no external field or with external magnetic field and change in temperature and pressure.

DC Magnetometry and AC Magnetometry are two types of Magnetometry used in research nowadays. Among several theories and procedures relating to Magnetometry our focus is mainly on identification and discrepancy between materials with superparamagnetic and super-spin glass behavior. Figure 3.4 provides the imagining of the chamber of the PPMS.

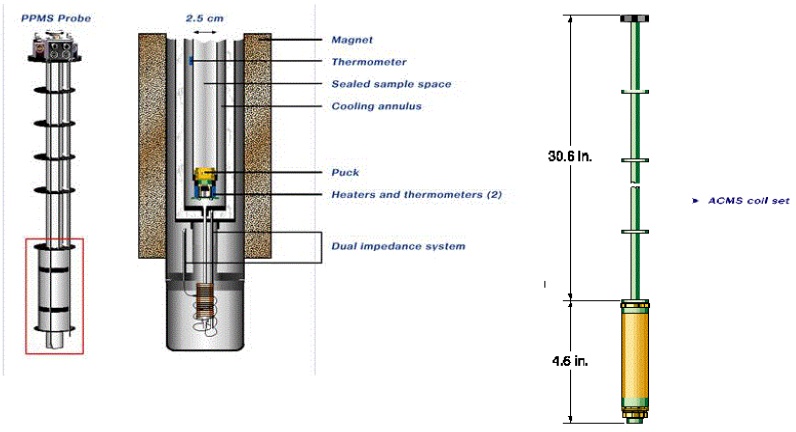

Figure 3.5– PPMS Inner-Chamber Configuration

In the beginning of the experiment DC-magnetization measurement was carried out, in which the sample was lowered into the coil assembly and direct current was applied. Then

cooling the sample via liquid helium to the starting temperature Zero-field-cooled (ZFC) measurements was taken. The coil assembly is raised and lowered by a motor system in order to produce a current, which is then measured. Then in the presence of a constant field with increasing temperature magnetization of the material is recorded. Similarly Field- Cooled (FC) measurements are carried out but the sample was cooled out in the presence of constant field. For FC and ZFC measurements the field used was set to 50 Oe with temperature beginning as low as 4 K and increasing to 140 K for both of the samples.

AC susceptibility measurement was also carried out for both of the sample. It involves a sample usually with some inherit magnetic properties in a constant DC magnetic field. The only difference with DC magnetometry is we add a small AC magnetic field to constant DC magnetic field. As a result the net superimposed field ends up having time dependence (this is due to the reason that AC field has time dependence). Hence, the magnetic moment of the sample creates a current in the induction coil. The moment that is created by the superimposed field is the AC magnetic moment. Also the temperature dependence of the sample was measured with different frequencies, with the oscillating magnetic field amplitude of 5 Oe, from 100 Hz up to 10000 Hz. The measurement data are then fit to mathematical model to determine the transition state of the material, whether super paramagnetic blocking (SPB) or superspin-glass freezing (SGG). Then using Vogel- Fulcher activation law and power activation law, we can see the observation time dependence. The temperature dependence of out of phase of susceptibility at different frequencies of 10nm sample is shown in fig 3.6.

Although mathematical model can give some difference between SPB and SGG, the data itself is hard to tell apart. So using the basis of magnetometry we use electron paramagnetic resonance, which easily differentiates the two phenomenon SPB, and SGG.

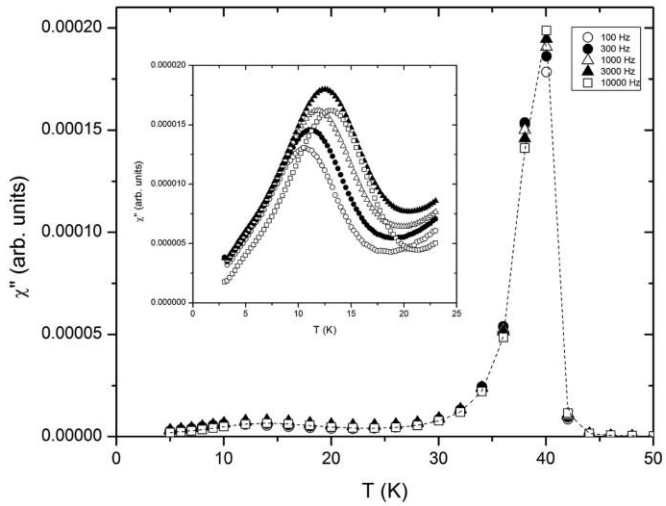

Fig 3.6: Temperature dependence of out of phase susceptibility.

Chapter 4: Results and Discussion

4.1 XRD Result

Samples of Mn3O4, 5 nm and 10 nm, were first characterized through the use of a single crystal x-ray diffractometer (figure 4.1 and 4.2)). We used a Bruker D8 Quest with a Photon 100 detector fitted with a molybdenum anode.

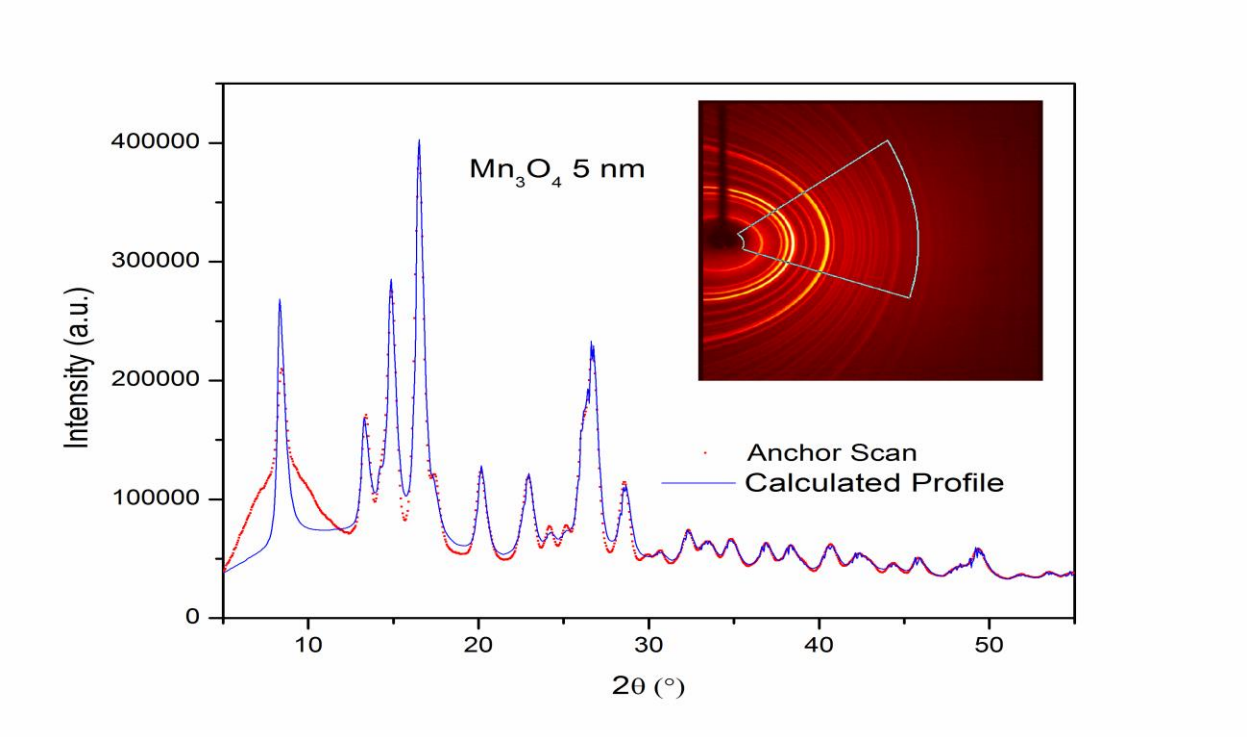

Fig 4.1: X-ray analysis of the Mn_3O_4 5 nm ensembles

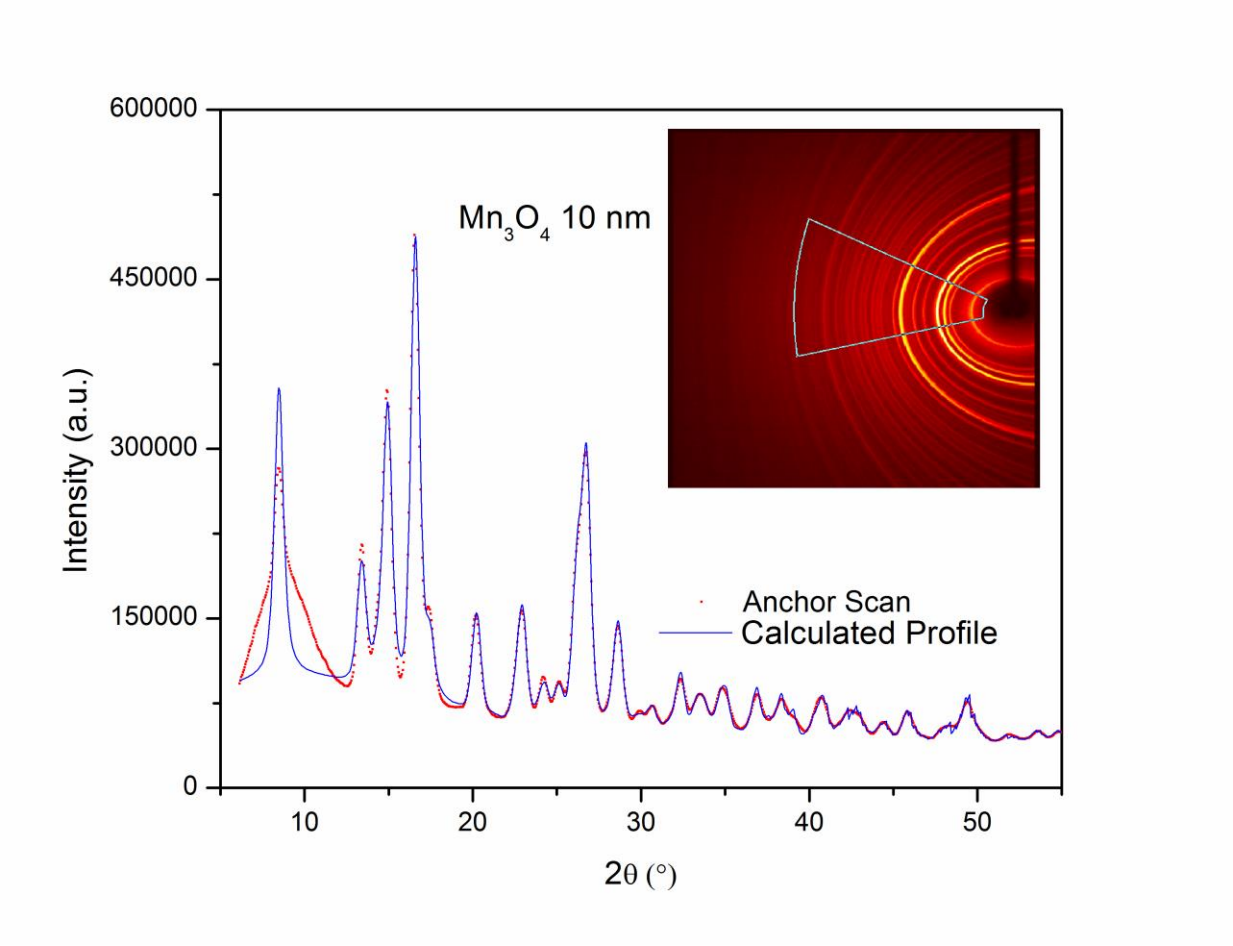

Fig 4.2: X-ray analysis of the Mn_3O_4 10 nm ensembles

The ring patterns were integrated to produce the peak pattern (red). The peak pattern fit properly with that of Mn3O4 (blue), though with the characteristic broadening as expected from nanoparticle ensembles. Utilizing the Scherrer equation, we calculated the average particle size to be 6.1 nm and 13.5 nm.

4.2 EPR Result

The first derivative of the EPR absorption spectra for the Mn3O4 nanoparticle of both 5nm and 10 nm was plotted intensity vs. temperature (Figure 4.3 and 4.4). We then isolated the absorption peak (the line center from the first derivative data) and plotted the absorption peaks vs. temperature (figure 4.4 and 4.5). The slope of the fitted line shows a distinct change in the 40 K – 50 K temperature range. The modulation frequency of the magnetic field for the EPR measurements is 100 kH

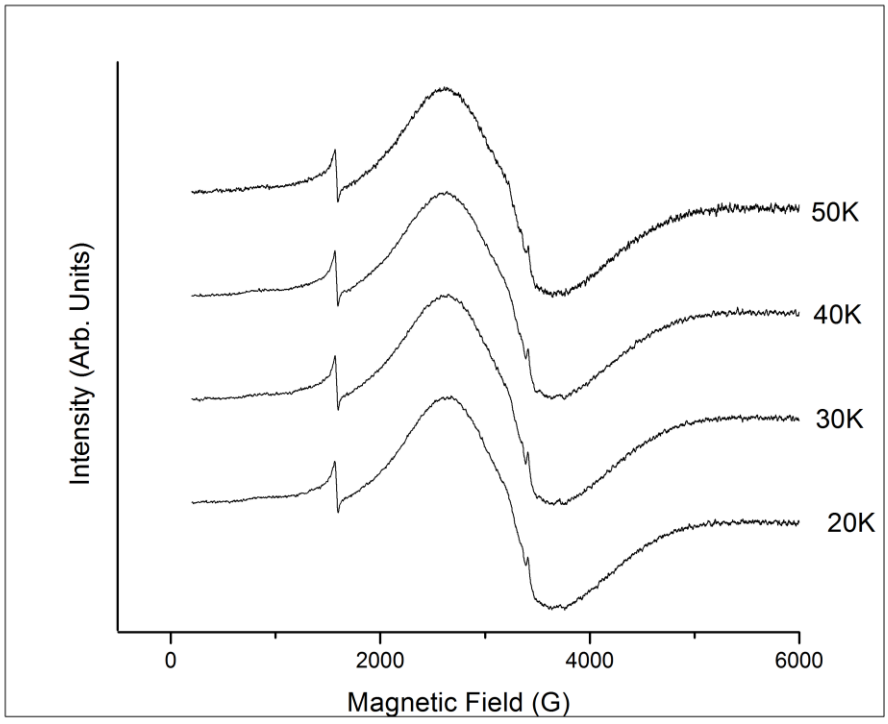

Figure 4.3 – 1st derivative of the absorption spectra of the Mn_3O_4 5 nm

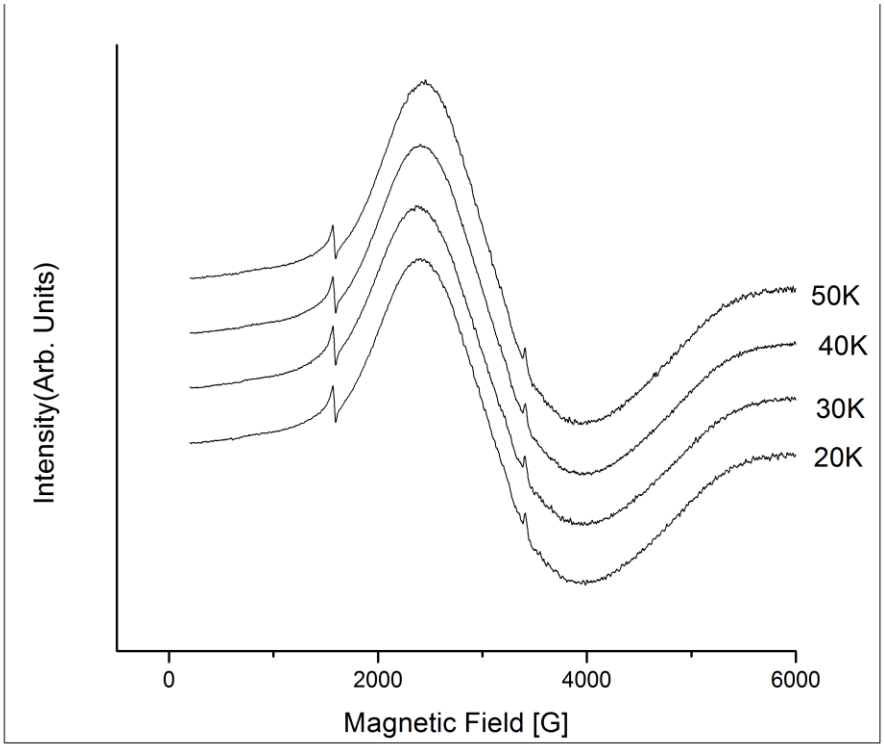

Figure 4.4 – 1st derivative of the absorption spectra of the Mn_3O_4 10 nm

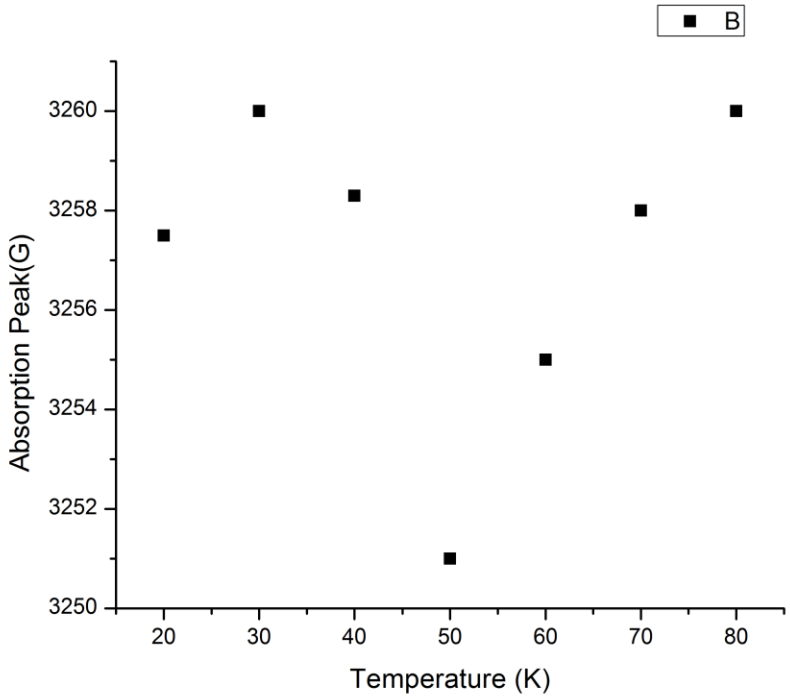

Fig 4.5: Absorption Peak vs Temperature for 5 nm.

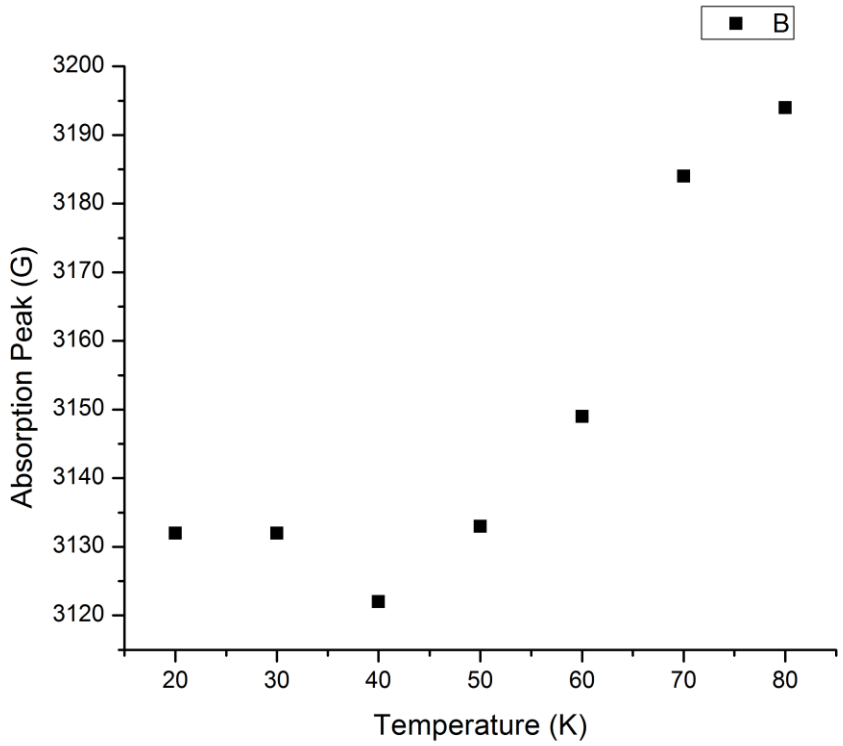

Fig 4.6: Absorption Peak vs Temperature for 10 nm.

In figure 4.6, we show the absorption peak change with temperature. In the 10 nm sample, we see a notable change in the behavior above and below 40 K, as indicative of the magnetic phase change. We see the same in the 5 nm samples, though shifted slightly to the right.

Chapter 5: Conclusions

Preliminary results verify the particle size of the magnetic nanoparticle ensembles via XRD and the Scherrer equation. The magnetic phase change is indicative by the changes in behavior as depicted by the absorption spectra via EPR, though there are notable differences between the two different size distributions. The Result is in match with the result of AC susceptibility measured using PPMS. The conclusion we can get from all experiment is when the nanoparticle size go on decreasing below the transition temperature also there is superparamagnetic behavior and we can verify superparamagnetic relaxation is the main cause of magnetic behavior in manganese oxide nanoparticles.

References

1] Natalie A. Frey and Shouheng Sun, Magnetic Nanoparticle for Information Storage Applications, CRC Press, (2010). (n.d.).

[2] J. L. Dormann, D. Fiorani and E. Tronc, Adv. Chem. Phys. 98, 283 (1997). (n.d.).

[3] Richard J. Harrison et al, Direct Imaging of Nanoscale Magnetic interactions in Minerals, Stanford University (2002). (n.d.).

[4] A. Ito, Journal of Bioscience and Bioengineering 100 (1), 1-11 (2005). (n.d.).

[5] S. X. Wang and A. M. Taratorin, Magnetic Information Storage Technology. (Academic, New York, 1999). (n.d.).

[6] K. E. Scarberry and E. B. Dickerson, Journal of the American Chemical Society 130 (31), 10258-62 (2008). (n.d.).

[7] P. Nikitin, Sensor Letters 5 (1), 296-299 (2007). (n.d.).

[8] An, G., Yu, P., & Xiao, M. (2008). Low-temperature synthesis of Mn3O4 nanoparticles loaded on multi-walled carbon nanotubes and their application in electrochemical capacitors. IOP Publishing, 19, 27th ser. doi:doi:10.1088/0957-4484/19/27/275709

[9] Al Saghee, F., Hasan, M., & Pasupulety, L. (1999). Low-temperature Synthesis of Hausmannite Mn3O4. Journal of Materials Science Letters, 18(3), 209-211. doi: 10.1023/A:1006620114539

[10] N. Ashcroft and D. Mermin, Soild State Physics. (Harcourt, Orlando, 1976). (n.d.).

[11] Journal of Materials Science Letters, 1999, Volume 18, Number 3, Page 209

F. A. Al Sagheer, M. A. Hasan, L. Pasupulety

[12] R. Bozorth, Ferromagnetism. (IEEE Press, New York, 1993). (n.d.).

[13] C. P. Bean and J. D. Livingston, J. Appl. Phys. 30 (1959). (n.d.)

[14] K. Binder and A. P. Young, Reviews of Modern Physics 58 (4), 801-976, (1986)

[15] P. Jonsson, Adv. Chem. Phys. **128**, 191-192.

[16] L. Neel, C. R. Hebd, Seances Acad. Sci. 5 (1949

[17] William Fuller Brown Jr., *Thermal Fluctuations of a Single-Domain Particle*, Physical Review 130 (5): 1677-1686 (1963

[18] S. Shtrikman and E. Wohlfarth, Phys. Lett. A 85, 467 (1981)

[19] J. L. Tholence, Solid State Comm. 35 (113) (1980)

[20] X. Chen, S. Bendata, O. Petracic, W. Kleemann, S. Sahoo, S. Cardoso, P. P. Freitas, Phys. Rev. B 72, 214439 (2005)

[21] C. Djurberg, P. Svedlindh, P. Norblad, M. F. Hansen, F. Bodker, S. Mørup, Phys. Rev. let. 79, 5154 (1997)

[22] (Cambridge Crystallographic Data Center, 2004).

Vita

Mahesh was born in Nepal, which is the small country in the South Asia. Mahesh completed his higher graduate study in Physics there but he again came to the United States for his Master Degree in Physics and served as a Graduate Student and Teaching Assistant at the University of Texas at El Paso. During this period he had his good academic record and did research works in the field of Nanotechnology and Material Science. He successfully completed his Master's thesis in Manganese Oxide nanoparticles. Now with his Master's in Physics from El Paso he is going to Clemson University, South Carolina for his PhD in Physics. He is going to continue his research work especially in the field of Biophysics and Condensed Matter of Physics.

Permanent address: Kavrepalanchok, Kavre-7

Nepal

This thesis/dissertation was typed by Mahesh Koirala.